Published in final edited form as:
J Neurochem. 2006 June ; 97(5): 1288–1300.

Abundance of triacylglycerols in ganglia and their depletion in diabetic mice: implications for the role of altered triacylglycerols in diabetic neuropathy

Hua Cheng, **Shaoping Guan**, and **Xianlin Han**
Division of Bioorganic Chemistry and Molecular Pharmacology, Department of Medicine, Washington University School of Medicine, St Louis, Missouri, USA

Abstract

Herein, we report the first study on the mass distribution and molecular species composition of abundant triacylglycerols (TAG) in ganglia. This study demonstrates five novel findings. First, unanticipated high levels of TAG were present in all examined ganglia from multiple species (e.g. mouse, rat and rabbit). Second, ganglial TAG mass content is location-dependent. Third, the TAG mass levels in ganglia are species-specific. Fourth, dorsal root ganglial TAG mass levels in streptozotocin-induced diabetic mice are dramatically depleted relative to those found in untreated control mice. Fifth, mouse ganglial TAG mass levels decrease with age although molecular species composition is not changed. Collectively, these results indicate that TAG is an important component of ganglia and may potentially contribute to pathological alterations in peripheral neuronal function in diabetic neuropathy.

Keywords

diabetic neuropathy; dorsal root ganglia; electrospray ionization mass spectrometry; peripheral nervous system; shotgun lipidomics; triacylglycerol

In addition to their well known role as the storage depots for metabolic energy, triacylglycerols (TAG) also possess many other biological functions, such as facilitating diacylglycerol as the biosynthesis precursor of phospholipids, protecting cells from sudden increases in fluxes of non-esterified fatty acids and acyl CoA, and insolating heat (for recent review see Coleman and Lee 2004). However, excessive TAG accumulation, commonly termed ‘lipotoxicity’, has been linked with deleterious changes including diabetes, obesity and atheroscrolesis (collectively termed the ‘metabolic syndrome’ (Unger 2002; Abelson and Kennedy 2004; Lazar 2005; Miranda *et al*. 2005a,b; Moller and Kaufman 2005), which is becoming a severe health problem in industrialized countries. TAG is mainly present in adipocytes, lipoproteins and small lipid droplets in multiple cells of some organs or tissues, such as liver and muscle, but is rarely present in cellular membranes in mammals (for recent reviews see Cullen 2003; Dolinsky *et al*. 2004; Londos *et al*. 2005).

Unlike the central nervous system, the peripheral nervous system (PNS) consists of ganglia (which are enriched with neuronal cell bodies) and nerve bundles (which comprise axons, myelin sheaths, vascular capillaries, collagens and other connective tissues). Each nerve bundle consists of many endoneuria (vascular layers surrounding individual nerve fibers), many perineuria (each of which arranges nerve fibers into ‘fascicles’) and an epineurium (which

Address correspondence and reprint requests to Xianlin Han, Ph.D., Division of Bioorganic Chemistry and Molecular Pharmacology, Department of Medicine, Washington University School of Medicine, Box 8020, 660 South Euclid Avenue, St. Louis, Missouri 63110, USA. E-mail: xianlin@wustl.edu.

binds ‘fascicles’ into an individual bundle) (Sunderland 1965; Rechthand and Rapoport 1987; Stolinski 1995).

Although some studies, especially those using histological techniques, have demonstrated that adipocytes are present in the peripheral nerve tissues, particularly in connective tissues between perineurium and epineurium layers (Sunderland 1945, 1965; Linington *et al*. 1980b; Dalziel 1989; Reina *et al*. 2002), the presence of adipocytes in the PNS, especially in ganglia, and its potential importance in pathological processes in the PNS have, for the most part, been neglected (Rechthand and Rapoport 1987; Stolinski 1995). To date, the quantitative distribution of TAG in the peripheral nerve tissues and the precise role(s) of these TAG molecular species present in the PNS remain unknown. The paucity of research interest in this area is due, in part, to current dogma that suggests that glucose is the sole fuel in the nervous systems and that TAG in the nervous systems is only present in very low amounts. In addition, there has been a lack of accurate techniques to perform lipid analyses of the PNS where sample sizes from suitable animal models may often be limited.

In recent times, a new field involving the large-scale study of lipids by integration of many modern techniques [e.g. electrospray ionization mass spectrometry (ESI/MS)], collectively known as lipidomics, is rapidly expanding following the tremendous progress made in genomics and proteomics (Han and Gross 2003; Lagarde *et al*. 2003). A very powerful technology in lipidomics has been developed, termed shotgun lipidomics, which is based on intrasource separation and multidimensional mass spectrometric array analyses (Han and Gross 2005a,b). Using this technology, individual molecular species of most major and many minor lipid classes, and over 95% of total lipid mass, can be quantitatively analyzed directly from lipid extracts of small amounts of biological samples (e.g. less than 2 mg of tissue). Thus, many experiments which were previously impractical can now be readily performed in an efficient and unbiased manner. This technology has already led to the discovery of many novel metabolic and biochemical paradigms underlying disease states and their corresponding diagnostic potential as biomarkers (Han *et al*. 2000, 2001, 2002, 2003, 2004a; Su *et al*. 2004; Han 2005).

This study was undertaken, using shotgun lipidomics, to determine whether TAG molecular species are present in ganglia and if so, what their compositions are. We demonstrate that TAG molecular species are present in unanticipated abundance in all examined ganglia from multiple examined species. The results indicate that ganglial TAG mass content is location-dependent. The study also demonstrates that the ganglial TAG mass contents from different species are quite variable. Moreover, TAG mass levels in the dorsal root ganglia (DRG) are the greatest in young mice and decrease measurably with age. To explore the potential role of the abundant ganglial TAG in peripheral nerve functions, we rendered mice diabetic by streptozotocin (STZ) treatment and determined the alterations in the DRG TAG mass and molecular species composition. Intriguingly, DRG TAG mass levels in STZ-induced diabetic mice were dramatically depleted relative to those found in the untreated controls. Collectively, this study identifies TAG as a major component in ganglia and suggests that it may fundamentally contribute to peripheral neuronal function in health and disease.

Materials and methods

Materials

Synthetic triheptadecenoyl glycerol (T17 : 1 TAG, used as an internal standard for ESI/MS analyses of ganglial TAG) was purchased from Nu-Chek Prep, Inc. (Elysian, MN, USA) and was quantitated by capillary gas chromatography after methanolysis (Gross 1984). All the solvents used for sample preparation and mass spectrometric analysis were obtained from Burdick and Jackson (Honeywell International Inc., Burdick and Jackson, Muskegon, MI,

USA). All other chemical reagents were at least analytical grade or the best grade available and were obtained from either Fisher Scientific (Pittsburgh, PA, USA) or Sigma-Aldrich Chemical Company (St. Louis, MO, USA), or as indicated.

Animal maintenance and treatment

Male New Zealand white rabbits (~1 kg body weight) were purchased from Myrtles Rabbitry, Inc. (Thompson Station, TN, USA). Male Sprague-Dawley rats (226−250 g body weight, approximately 2 months of age) were purchased from Charles River Laboratories, Inc. (Wilmington, MA, USA). Female mice on a C57BL/6 background at the indicated ages were purchased from The Jackson Laboratory (Bar Harbor, ME, USA). Animals used for long-term studies were housed in a full barrier facility with a 12 h light/dark cycle and maintained on standard chow (Diet 5053; Purina Inc., St. Louis, MO, USA).

Mouse diabetes was induced by a single intravenous injection (in the tail vein) of streptozotocin at 4 months of age (160 mg/kg body weight in 0.1 mL of 0.1 M citrate buffer, pH 4.5) (Jansson *et al*. 1989). Control mice received citrate buffer (0.1 mL) alone. Diabetes was confirmed within 48 h by blood glucose levels > 3 mg/mL as measured by chemstrips (bG, Boehringer-Mannheim, Indianapolis, IN, USA). Blood glucose levels were checked daily in the morning. All animal procedures were performed in accordance with the 'Guide for the Care and Use of Laboratory Animals' (National Academy of Science 1996) and were approved by the 'Animals Studies Committee' at Washington University.

Preparation of lipid extracts from animal ganglia

Animals were killed by asphyxiation with carbon dioxide and decapitated. After removal of the skin and muscle around the neck of each animal, pairs of cervical nerves were pulled out after each cervical vertebra was carefully removed. Cervical dorsal root ganglia (DRG) were dissected after the attached nerve bundle was cut away from each of the pulled cervical nerves. Thoracic DRG were similarly dissected from the designated locations. Prevertebral superior mesenteric ganglia (SMG) were dissected free of adjacent tissues following the instruction previously described (Schmidt *et al*. 1983). Paravertebral superior cervical ganglia (SCG) were similarly dissected free of adjacent tissues from the designated locations. The ganglia were immediately frozen in liquid nitrogen and stored at −80°C (< 1 month) before lipid extraction. Ganglial tissues (1−5 mg) were cut into very small pieces prior to homogenization in 200 μL of ice-cold LiCl solution (50 mM) using a Potter-Elvehjem tissue grinder (Fisher Scientific, Pittsburgh, PA, USA) for at least 5 min on ice. Protein assays on the homogenates were performed. An internal standard (T17 : 1 TAG, 10 nmol/mg protein) for ESI/MS analyses of TAG molecular species was added to each individual homogenate after it was transferred to a borosilicate glass culture tube (size 16 × 100 mm).

Lipids from each homogenate were extracted by a modified Bligh and Dyer procedure (Bligh and Dyer 1959) as described previously (Han and Gross 2001; Han *et al*. 2004a). Specifically, to each individual homogenate, 4 mL chloroform/methanol (1 : 1, v/v) and 1.6 mL LiCl solution (50 mM) were added. The extraction mixtures were vortexed and centrifuged at 2500 r.p.m. for 5 min. The chloroform layer of each extract mixture was carefully removed and saved. An additional 2 mL chloroform was added into the MeOH/aqueous layer of each test tube. After centrifugation, the chloroform layer from each individual sample was combined and dried under a nitrogen stream. Each individual residue was then resuspended in 4 mL chloroform/methanol (1 : 1), back-extracted against 1.8 mL LiCl aqueous solution (10 mM), and the extract was dried as described above. Each individual residue was resuspended in approximately 1 mL chloroform and filtered with a 0.2 μm polytetrafluoroethylene (PFTE) syringe filter. Finally, each individual residue was reconstituted with a volume of 1 mL/mg protein (which was based on the original protein content of the samples as determined from protein assays)

in 1 : 1 chloroform/methanol. The lipid extracts were finally flushed with nitrogen, capped, and stored at −20°C for ESI/MS analyses (typically conducted within 1 week).

Instrumentation

A triple-quadrupole mass spectrometer (ThermoElectron TSQ Quantum Ultra, San Jose, CA, USA), equipped with an electrospray ion source and operated under an XCALIBUR operational software system, was used in the study as previously described (Han *et al*. 2004b). Briefly, the spray voltage was maintained at −3.2 kV in the positiveion mode. An offset voltage on the ion transfer capillary was set to 17 V in the positive-ion mode. The temperature along the ion transfer capillary was maintained at 250°C. The sheath gas (nitrogen) pressure was 13.8 kPa. The collision gas (argon) pressure and the collision energy were set at 1.0 mTorr and 32 eV, respectively, for tandem mass spectrometry in the neutral loss (NL) mode.

Mass spectrometric analyses of ganglial triacylglycerols

The lipid extract of each ganglial sample was further diluted approximately 20-fold immediately prior to infusion and lipid analysis. LiOH (50 nmol/mg protein) was added just prior to performing ganglial TAG analyses in the positive-ion mode. The lithium ions were used to facilitate the analyses of TAG molecular species (Han and Gross 2005a), whereas the hydroxide ions facilitated the intrasource separation of electrically neutral lipids (e.g. TAG and choline glycerophospholipids) from anionic lipids and weak zwitterionic lipids, such as ethanolamine glycerophospholipids (Han and Gross 2005a,b; Han *et al*. 2006). The diluted lipid extract solution was directly infused into the ESI ion source at a flow rate of 4 μL/min with a Harvard syringe pump.

Identification and quantitation of individual TAG molecular species were conducted using a two-dimensional (2D) mass spectrometric technique, as described previously (Han and Gross 2001; Han *et al*. 2004b). Briefly, all the MS and tandem MS traces of ganglial TAG in the 2D mass spectrum were automatically acquired by a custom sequence sub-routine operated under the XCALIBUR software with a 1 or 2 min period of signal averaging in the profile mode for each MS or tandem MS trace. For tandem mass spectrometry in the positive-ion neutral loss (NL) mode, both the first and third quadrupoles were co-ordinately scanned with a mass difference (i.e. neutral loss) corresponding to the neutral loss of a non-esterified fatty acid (representing a building block of TAG molecular species) from TAG molecular species, while collisional activation was performed in the second quadrupole. Then, 2D mass spectrometric array analyses were performed. Through identification of the cross peaks from the building blocks with each individual lithiated TAG molecular ion peak in the first dimensional mass spectral trace, the identities of the TAG molecular ion peaks in the 2D spectrum were identified. After corrections for the differences in ^{13}C isotopomer distributions and in response factors of different TAG molecular species, each identified TAG molecular species was quantitated within 10% of experimental error (Han and Gross 2001). Data processing of two-dimensional mass spectrometric analyses, including ion peak selection, data transferring, peak intensity comparison and quantitation, was conducted as previously described (Han and Gross 2001; Han *et al*. 2004b) using self-programmed MicroSoft Excel macros.

Miscellaneous

Protein concentration was determined with a bicinchroninic acid protein assay kit (Pierce, Rockford, IL, USA) using bovine serum albumin as a standard. Data from ganglial samples were normalized to the protein content of each sample, and all data are presented as the mean ± SEM of a minimum of four separate animals. Statistical differences between mean values were determined by nested ANOVA.

Results

Presence of abundant TAG in rat ganglia

Shotgun lipidomics analyses of lipid extracts from prevertebral SMG in the positive-ion mode of ESI/MS after intrasource separation demonstrated very abundant ion clusters at *m/z* 837.7, 863.8, 879.8, 887.8 and 903.8 between *m/z* 800 and 980 (Fig. 1a). These abundant ion peaks were identified as the lithium adducts of TAG molecular species by 2D ESI/MS analyses of the building blocks of TAG (i.e. all potentially naturally-occurring fatty acids) (Han and Gross 2005b) (Fig. 2). For example, the ion peak at *m/z* 889.8 was predominantly crossed with the TAG building blocks of 18 : 2 FA (NL280), 18 : 1 FA (NL282), 18 : 0 FA (NL284), 20 : 2 FA (NL308) and 20 : 0 FA (NL312) along with many low-abundance crossing peaks such as 16 : 1 FA (NL254), 16 : 0 FA (NL256), 18 : 3 FA (NL278), 20 : 1 FA (NL310) and 20 : 4 FA (NL304) (highlighted by the broken line in Fig. 2). From these crossing peaks, we identified the four abundant isobaric TAG molecular species, 18 : 0/18 : 2/18 : 2, 18 : 1/18 : 1/18 : 2, 16 : 0/18 : 0/20 : 4 and 16 : 0/18 : 2/20 : 2 TAG, and several low abundance TAG species such as 18 : 0/17 : 1/19 : 3, 16 : 1/18 : 2/20 : 1 and 17 : 2/17 : 2/20 : 0 TAG. Over 100 TAG molecular species, each of which was at least > 0.01 mol% of the total TAG mass in abundance, were identified directly from the lipid extracts of rat SMG.

After identification, individual SMG TAG molecular species were quantitated after corrections for ^{13}C isotopomer difference and ionization response factor differences relative to the selected internal standard, as described previously (Han and Gross 2001), with approximately 10% accuracy. The total mass content of rat SMG TAG was 543.3 ± 44.6 nmol/mg protein. The mass contents of rat SMG TAG molecular species were determined by 2D ESI/MS analyses and tabulated (Table 1). From the 2D ESI/MS analyses, it was also found that the most abundant fatty acyl moiety in rat SMG TAG was oleoyl, accounting for 30.9 mol% of the total acyl chains, followed by linoleoyl, palmitoyl and stearoyl moieties, representing 25.0, 23.4 and 6.9 mol%, respectively (Table 1). Among the fatty acyl moieties of the rat SMG TAG, polyunsaturated fatty acyl chains (containing two or more double bonds) accounted for 30.6 mol% of the total acyl chains; fatty acyl chains containing an odd number of carbons accounted for 2.7 mol% of the total fatty acyl chains, and the TAG acyl chains consisting of 20 or more carbons accounted for 4.0 mol% of the total fatty acyl chains (Table 1).

The presence of abundant TAG in the rat ganglia was also demonstrated by shotgun lipidomic analyses of lipid extracts from all other examined ganglial locations, including paravertebral SCG (Fig. 1b), thoracic DRG (Fig. 1c) and cervical DRG (Fig. 1d). Interestingly, the total mass contents of TAG were dramatically increased in the order of cervical DRG, thoracic DRG, SCG and SMG (Table 1), as demonstrated by the increased ratios of the peak intensities of TAG molecular species versus the peak intensity of the selected internal standard (Fig. 1). In addition, the profiles of individual TAG molecular species were quite varied in different ganglial locations. Specifically, the dominant lithiated TAG ion peaks were at *m/z* 861.8, 863.8, 887.8 and 889.8 in SMG, at *m/z* 863.8, 887.8 and 889.8 in SCG, at *m/z* 863.8, 865.8 and 889.8 in thoracic DRG, and at *m/z* 865.8 in cervical DRG (Fig. 1). These results suggest that the metabolic/catabolic pathways of TAG at distinct ganglial locations might be quite different. This was further supported by the different compositions of TAG acyl chain moieties containing odd numbered carbons (which varied from 2.7 mol% in SMG to 5.7 mol% in cervical DRG) and those containing polyunsaturated acyl chains (which varied from 35.1 mol % in SCG to 22.0 mol% in thoracic DRG) (Table 1).

Presence of abundant TAG in other examined mammalian ganglia

To identify whether the presence of abundant TAG in rat ganglia is a general phenomenon in mammals, we examined the presence of ganglial TAG in other species (including mouse and

rabbit) using shotgun lipidomics. ESI mass spectrometric analyses of lipid extracts of these mammalian DRG again demonstrated the presence of abundant TAG (Fig. 3). Quantitation of the identified TAG molecular species yielded a total TAG mass of 15.0 ± 1.4 nmol/mg protein in cervical DRG of rabbit and 49.9 ± 5.3 nmol/mg protein in cervical DRG of mice at 5 months of age. The profile of TAG molecular species of mouse cervical DRG is comparable with that of rat cervical DRG (compare Fig. 3a with Fig. 3b), but the profile of TAG molecular species of rabbit cervical DRG is quite different from those of either species (Fig. 3c).

Ganglial TAG mass and composition are age-dependent

Next, using mice as an animal model, the age dependence of cervical DRG TAG mass and fatty acyl chain composition was examined. Shotgun lipidomics analyses demonstrated a modest age-dependent change in mouse DRG TAG mass, which decreased from 55.5 ± 2.4 nmol/mg protein at 2 months of age, to 49.9 ± 5.3 nmol/mg protein at 5 months of age ($p < 0.05$) and to 41.7 ± 3.0 nmol/mg protein at 8 months of age ($p < 0.001$) (Table 2). The mass contents of each individual TAG molecular species and individual acyl chain moiety were also essentially decreased (Table 2). In addition, shotgun lipidomics analyses of mouse DRG TAG at 2 months of age demonstrated that 5.7 ± 0.2 mol% of the TAG molecular species present contained fatty acyl chains with odd numbered carbons, 18.8 ± 1.0 mol% of the acyl chains possessed two or more double bonds, and 4.7 ± 0.4 mol% of fatty acyl chains were composed of 20 or more carbons. Relative compositions of these specific acyl chain groups were independent of age (within experimental error) (Table 2). Intriguingly, these compositions present in mouse cervical DRG TAG were comparable with those present in rat cervical DRG TAG (i.e. 5.7 ± 1.1, 23.1 ± 2.9 and 5.9 ± 0.9 mol% of fatty acyl chains containing odd numbered carbons, two or more double bonds and 20 or more carbons, respectively, at 2 months of age; Table 1).

Depletion of TAG in diabetic mouse DRG

To explore the potential role of the abundant ganglial TAG in peripheral nerve functions, alterations in ganglial TAG mass and molecular species composition in a diabetic animal model were examined. Diabetes was induced in mice (about 4 months of age) by STZ treatment (Jansson *et al*. 1989) and the mice were killed after an onset of diabetes for 4 weeks (i.e. at about 5 months of age). TAG mass and molecular species compositions of cervical DRG from these diabetic mice were quantitatively analyzed by shotgun lipidomics. Positive-ion ESI mass spectrometric analyses demonstrated substantially lower ion peak intensities of TAG molecular species in diabetic mouse cervical DRG in comparison with those obtained from the cervical DRG of the age-matched control mice (Fig. 4). Conversely, other lipid components (such as phosphatidylcholine and sphingomyelin molecular species), as demonstrated in the spectra, were unchanged within experimental error (Fig. 4).

The dramatic decreases in TAG ion peak intensities after induction of diabetes were further substantiated by analyses of the composition of TAG fatty acyl moieties (Fig. 5a) and the mass contents of all TAG individual molecular species (Table 3). Figure 5(a) shows that all of the fatty acyl chains in the TAG pool of diabetic mouse cervical DRG were substantially depleted in comparison with those in the control. However, a comparison of the compositions of TAG fatty acyl chains in diabetic versus control clearly demonstrated that the losses of the different fatty acyl chains in the DRG TAG pool induced by STZ treatment were not identical (Fig. 5b). For example, 18 : 2, 18 : 0 and 22 : 6 acyl chains were more resistant to depletion from DRG TAG pools following an induction of diabetes and thus, the relative percentages of these acyl moieties were dramatically increased in the composition of the remaining TAG molecular species (Fig. 5b). The composition of acyl chains 14 : 0, 15 : 0, 16 : 0 and 20 : 4 were essentially unchanged (Fig. 5b), although the absolute mass contents of these acyl chains decreased in diabetic states relative to those in controls (Fig. 5a), indicating a proportional loss of these

moieties relative to the average depletion whereas all other acyl components suffered a loss greater than a proportional value. These results indicate that those acyl chains that are either polyunsaturated (two or more double bonds) or saturated are less affected by STZ treatment.

Discussion

Quantitative analyses of cellular lipids in the PNS have been the topic of many previous studies in neurochemistry (Linington *et al*. 1980a; Yao *et al*. 1981; Fressinaud *et al*. 1986, 1987a,b; Ganser *et al*. 1988a,b), although these studies mainly quantified the fatty acyl chain profiles of total lipids, or individual lipid classes in different PNS tissues, or the cultured cells from PNS nerves. Alterations of diacylglycerol mass content and phospholipid molecular species composition in sciatic nerve from STZ-induced diabetic rats have been reported (Zhu and Eichberg 1990, 1993). The presence of adipose tissue has been demonstrated in the nerve bundles, particularly in connective tissues between the perineurium and epineurium layers (Sunderland 1945, 1965; Linington *et al*. 1980b; Dalziel 1989; Reina *et al*. 2002), although quantitative data regarding fat alterations in the PNS (particularly at the level of lipid molecular species) are still lacking. However, the enzymes associated with fat metabolism in the PNS have been found to be closely involved in peripheral nerve development (Verheijen *et al*. 2003), after nerve injury (Huey *et al*. 2002; Xiao *et al*. 2002) and during neuronal atrophy in the STZ-induced diabetic state (Eliasson and Hughes 1960; Ferreira *et al*. 2002). Furthermore, knowledge of the presence and function of adipose tissue in ganglia is quite limited (Dalziel 1989; Czaja *et al*. 2002a,b).

Our study reports the first detailed determination of the mass distribution and molecular species composition of TAG in ganglia and demonstrates several novel findings. TAG molecular species were abundant in all examined ganglia (prevertebral superior mesenteric ganglia, paravertebral superior cervical ganglia, thoracic dorsal root ganglia and cervical dorsal root ganglia) from multiple species (mouse, rat and rabbit). The TAG mass levels of the ganglia varied substantially in different species. Mouse DRG TAG mass levels were age-dependent (i.e. DRG TAG mass decreases with aging) but the fatty acyl composition of DRG TAG remained unchanged with age. Intriguingly, DRG TAG mass levels in STZ-induced diabetic mice were dramatically depleted compared with those found in the counterparts of untreated control mice. These results indicate that TAG is a major component of ganglia and may significantly contribute to normal peripheral neuronal function.

Long-term changes in adipose tissues have been found in multiple human diseases such as HIV adipose redistribution syndrome and Crohn's disease (Pond 2001). Due to a lack of studies on functions of the PNS adipocytes, the precise roles of abundant TAG in ganglia remain unknown. However, at least three potential roles can be postulated. First, the ganglial TAG may be directly involved in local lipid metabolic pathways, and the TAG could serve as an energy depot as well as a pool for supplying metabolites such as acyl CoA for the peripheral neurons. The expression of lipoprotein lipase in Schwann cells (Huey *et al*. 1998) and in the sciatic nerve (Huey *et al*. 2002) directly indicates PNS TAG as a source of fatty acids. In this regard, a recent study on peripheral nerve development has found a local regulation of fat metabolism in the peripheral nerves (Verheijen *et al*. 2003), supporting an important role for ganglial TAG. In addition to their role in energy storage, adipocytes can also serve as an endocrine organ, due to their production and secretion of adipokines, to regulate energy homeostasis and insulin action in many different tissues including brain (Saltiel and Kahn 2001). Therefore, the PNS TAG levels may serve as a sensor for the production and secretion of adipokines, such as leptin and adiponectin, or other as yet undescribed factors. Due to the insulative physical properties of TAG, these interfascicular adipose tissues or oily droplets may act as a physical buffer or cushion for the fasciculi to protect the peripheral nerves. This particular function of TAG would be analogous to that of the skull and the spinal vertebrae for

the protection of the central nervous system. Therefore, it can be theorized that the peripheral nerves would function abnormally or potentially degenerate if the content and/or composition of ganglial TAG were altered.

Following this line of reasoning, it is particularly interesting that ganglial TAG mass levels decrease with aging and are substantially depleted in the diabetic state. Lower TAG mass levels in aged ganglia coincide with the reduction of peripheral nerve sensation in older populations. Whether the loss of nerve conduction or other neuropathies in diabetic animals (Sima *et al*. 2000) are associated with the depletion of ganglial TAG in the diabetic state remains unknown. However, it can be speculated that the severe depletion of ganglial TAG molecular species in diabetes could contribute to the pathogenesis of diabetic neuropathy as discussed above. Surprisingly, the depletion of TAG in ganglia is in contrast to the accumulation of fat in most of the other organs during the development of diabetes (Finck *et al*. 2002, 2003; Han *et al*. 2005), suggesting that a bi-directional TAG redistribution occurs in the pathogenesis of diabetes. Thus, inhibition of fat redistribution in the diabetic state, if possible, may be able to provide a therapy to prevent or cure the disease.

Another important finding/observation of particular interest is the abundance of polyunsaturated fatty acyl moieties, including linoleate, arachidonate and docosahexaenoate (the essential fatty acids) present in the ganglial TAG pool. It is well known that polyunsaturated fatty acids serve many essential neuronal functions, such as synaptic plasticity, memory and as mediators of signal transduction cascades, and also greatly contribute to many neuropathological conditions such as stroke, epilepsy and Alzheimer's disease (Han *et al*. 2001; Bazan 2003). Thus, the storage of a large amount of essential fatty acids in the ganglial TAG pool could facilitate a depot to supply these components for normal neuronal functions. Even in the diabetic state, such a reservoir of essential fatty acids is apparently preserved since other fatty acyl chains are preferentially lost from the ganglial TAG pool.

Finally, the quantity of fatty acyl moieties containing odd numbered carbons is quite large in comparison with other animal tissues or organs (Newberry *et al*. 2003; Han *et al*. 2004a,b), accounting for up to 6 mol% of total ganglial TAG acyl chains. Such a high percentage of acyl chains with odd numbered carbons in the TAG pool is quite unusual in other organs (Newberry *et al*. 2003; Han *et al*. 2004a). Although the presence of the abundant acyl chains containing odd numbered carbons apparently indicates the active involvement of α-oxidation for the production of heat through a peroxisomal process in fat metabolism in the peripheral nerves (Su *et al*. 2004), the precise role(s) of such a process in the PNS remains unknown.

Collectively, this study provides the first detailed characterization of the TAG mass distributions and TAG molecular species compositions in ganglia. Many unanswered questions remain, such as the exact role(s) of the abundant TAG in ganglia, the metabolism and utilization of ganglial TAG, the biochemical mechanism(s) underlying the depletion of ganglial TAG in the diabetic state, and the relationship between the depletion of ganglial TAG and diabetic neuropathy. For example, loss of ganglial TAG could result from accelerated degradation or insufficient biosynthesis, or both, and therefore, many enzymes and regulatory factors in biosynthesis and degradation of TAG (Coleman and Lee 2004) may be involved in the depletion of ganglial TAG in the diabetic state. Investigations to answer these questions and other related topics are underway in our laboratory to provide new insights into peripheral nerve function and PNS diseases such as diabetic neuropathy.

Acknowledgements

This work was supported by National Institute on Aging Grant R01 AG23168 and the Neurosciences Education and Research Foundation. The authors are grateful to Dr Christopher M. Jenkins for his comments and to Dr Kui Yang for her technical help.

Abbreviations used

DRG, dorsal root ganglion or ganglia; ESI, electrospray ionization; FA, fatty acid or fatty acyl chain; m:n, acyl chain containing m carbons and n double bonds; MS, mass spectrometry; NL, neutral loss; PFTE, polytetrafluoroethylene; PNS, peripheral nervous system; SCG, superior cervical ganglion or ganglia; SMG, superior mesenteric ganglion or ganglia; STZ, streptozotocin; TAG, triacylglycerol; Tm:n TAG, tri m:n glycerol.

References

Abelson P, Kennedy D. The obesity epidemic. Science 2004;304:1413. [PubMed: 15178768]

Bazan NG. Synaptic lipid signaling: Significance of polyunsaturated fatty acids and platelet-activating factor. J. Lipid Res 2003;44:2221–2233. [PubMed: 13130128]

Bligh EG, Dyer WJ. A rapid method of total lipid extraction and purification. Can. J. Biochem. Physiol 1959;37:911–917. [PubMed: 13671378]

Coleman RA, Lee DP. Enzymes of triacylglycerol synthesis and their regulation. Prog. Lipid Res 2004;43:134–176. [PubMed: 14654091]

Cullen P. Triacylglycerol-rich lipoproteins and atherosclerosis – where is the link? Biochem. Soc. Trans 2003;31:1080–1084. [PubMed: 14505484]

Czaja K, Kraeling R, Klimczuk M, Franke-Radowiecka A, Sienkiewicz W, Lakomy M. Distribution of ganglionic sympathetic neurons supplying the subcutaneous, perirenal and mesentery fat tissue depots in the pig. Acta Neurobiol. Exp. (Wars.) 2002a;62:227–234. [PubMed: 12659288]

Czaja K, Lakomy M, Kaleczyc J, Barb CR, Rampacek GB, Kraeling RR. Leptin receptors, npy, and tyrosine hydroxylase in autonomic neurons supplying fat depots in a pig. Biochem. Biophys. Res. Commun 2002b;293:1138–1144. [PubMed: 12051778]

Dalziel K. The nervous system and adipose tissue. Clin. Dermatol 1989;7:62–77. [PubMed: 2691052]

Dolinsky VW, Gilham D, Alam M, Vance DE, Lehner R. Triacylglycerol hydrolase: Role in intracellular lipid metabolism. Cell. Mol. Life Sci 2004;61:1633–1651. [PubMed: 15224187]

Eliasson SG, Hughes AH. Cholesterol and fatty acid synthesis in diabetic nerve and spinal cord. Neurology 1960;10:143–147. [PubMed: 13819924]

Ferreira LD, Huey PU, Pulford BE, Ishii DN, Eckel RH. Sciatic nerve lipoprotein lipase is reduced in streptozotocin-induced diabetes and corrected by insulin. Endocrinology 2002;143:1213–1217. [PubMed: 11897675]

Finck BN, Lehman JJ, Leone TC, et al. The cardiac phenotype induced by pparα overexpression mimics that caused by diabetes mellitus. J. Clin. Invest 2002;109:121–130. [PubMed: 11781357]

Finck BN, Han X, Courtois M, Aimond F, Nerbonne JM, Kovacs A, Gross RW, Kelly DP. A critical role for pparα-mediated lipotoxicity in the pathogenesis of diabetic cardiomyopathy: Modulation by dietary fat content. Proc. Natl Acad. Sci. USA 2003;100:1226–1231. [PubMed: 12552126]

Fressinaud C, Rigaud M, Vallat JM. Fatty acid composition of endoneurium and perineurium from adult rat sciatic nerve. J. Neurochem 1986;46:1549–1554. [PubMed: 3958717]

Fressinaud C, Vallat JM, Rigaud M, Leboutet MJ. Analysis of unsaturated fatty acids of endoneurium and perineurium from normal and degenerating rat sciatic nerve. Morphological correlations. J. Neurol. Sci 1987a;81:85–92. [PubMed: 3681343]

Fressinaud C, Vallat JM, Durand J, Archambeaud-Mouveroux F, Rigaud M. Changes in composition of endoneurial and perineurial fatty acids during glycerol-induced wallerian degeneration and regeneration in the sciatic nerve of the adult rat. J. Neurochem 1987b;49:797–801. [PubMed: 3612125]

Ganser AL, Kerner AL, Brown BJ, Davisson MT, Kirschner DA. A survey of neurological mutant mice. I. Lipid composition of myelinated tissue in known myelin mutants. Dev. Neurosci 1988a;10:99–122. [PubMed: 3402360]

Ganser AL, Kerner AL, Brown BJ, Davisson MT, Kirschner DA. A survey of neurological mutant mice. Ii. Lipid composition of myelinated tissue in possible myelin mutants. Dev. Neurosci 1988b;10:123–140. [PubMed: 3402356]

Gross RW. High plasmalogen and arachidonic acid content of canine myocardial sarcolemma: a fast atom bombardment mass spectroscopic and gas chromatography-mass spectroscopic characterization. Biochemistry 1984;23:158–165. [PubMed: 6419772]

Han X. Lipid alterations in the earliest clinical stage of Alzheimer's disease: Implication of the role of lipids in the pathogenesis of Alzheimer's disease. Curr. Alzheimer Res 2005;2:65–77. [PubMed: 15977990]

Han X, Gross RW. Quantitative analysis and molecular species fingerprinting of triacylglyceride molecular species directly from lipid extracts of biological samples by electrospray ionization tandem mass spectrometry. Anal. Biochem 2001;295:88–100. [PubMed: 11476549]

Han X, Gross RW. Global analyses of cellular lipidomes directly from crude extracts of biological samples by esi mass spectrometry: a bridge to lipidomics. J. Lipid Res 2003;44:1071–1079. [PubMed: 12671038]

Han X, Gross RW. Shotgun lipidomics: Electrospray ionization mass spectrometric analysis and quantitation of the cellular lipidomes directly from crude extracts of biological samples. Mass Spectrom. Rev 2005a;24:367–412. [PubMed: 15389848]

Han X, Gross RW. Shotgun lipidomics: Multi-dimensional mass spectrometric analysis of cellular lipidomes. Expert Rev. Proteomics 2005b;2:253–264. [PubMed: 15892569]

Han X, Abendschein DR, Kelley JG, Gross RW. Diabetes-induced changes in specific lipid molecular species in rat myocardium. Biochem. J 2000;352:79–89. [PubMed: 11062060]

Han X, Holtzman DM, Mckeel DW, Jr. Plasmalogen deficiency in early Alzheimer's disease subjects and in animal models: Molecular characterization using electrospray ionization mass spectrometry. J. Neurochem 2001;77:1168–1180. [PubMed: 11359882]

Han X, Holtzman DM, Mckeel DW, Jr, Kelley J, Morris JC. Substantial sulfatide deficiency and ceramide elevation in very early Alzheimer's disease: Potential role in disease pathogenesis. J. Neurochem 2002;82:809–818. [PubMed: 12358786]

Han X, Fagan AM, Cheng H, Morris JC, Xiong C, Holtzman DM. Cerebrospinal fluid sulfatide is decreased in subjects with incipient dementia. Ann. Neurol 2003;54:115–119. [PubMed: 12838527]

Han X, Cheng H, Mancuso DJ, Gross RW. Caloric restriction results in phospholipid depletion, membrane remodeling and triacylglycerol accumulation in murine myocardium. Biochemistry 2004a;43:15, 584–15, 594.

Han X, Yang J, Cheng H, Ye H, Gross RW. Towards fingerprinting cellular lipidomes directly from biological samples by two-dimensional electrospray ionization mass spectrometry. Anal. Biochem 2004b;330:317–331. [PubMed: 15203339]

Han X, Yang J, Cheng H, Yang K, Abendschein DR, Gross RW. Shotgun lipidomics identifies cardiolipin depletion in diabetic myocardium linking altered substrate utilization with mitochondrial dysfunction. Biochemistry 2005;44:16, 684–16, 694.

Han X, Yang K, Yang J, Fikes KN, Cheng H, Gross RW. Factors influencing the electrospray intrasource separation and selective ionization of glycerophospholipids. J. Am. Soc. Mass Spectrom 2006;17:264–274. [PubMed: 16413201]

Huey PU, Marcell T, Owens GC, Etienne J, Eckel RH. Lipoprotein lipase is expressed in cultured Schwann cells and functions in lipid synthesis and utilization. J. Lipid Res 1998;39:2135–2142. [PubMed: 9799799]

Huey PU, Waugh KC, Etienne J, Eckel RH. Lipoprotein lipase is expressed in rat sciatic nerve and regulated in response to crush injury. J. Lipid Res 2002;43:19–25. [PubMed: 11792718]

Jansson L, Eizirik DL, Sandler S. Terbutaline decreases the blood flow of the pancreatic islets but does not reduce the diabetogenic action of streptozotocin in the rat. Eur. J. Pharmacol 1989;161:79–83. [PubMed: 2656272]

Lagarde M, Geloen A, Record M, Vance D, Spener F. Lipidomics is emerging. Biochim. Biophys. Acta 2003;1634:61. [PubMed: 14643793]

Lazar MA. How obesity causes diabetes: Not a tall tale. Science 2005;307:373–375. [PubMed: 15662001]

Linington C, Neuhoff V, Waehneldt TV. The lipid and glycoprotein composition of peripheral-nervous-system myelin subfractions isolated by zonal centrifugation. Biochem. Soc. Trans 1980a;8:69–70.

Linington C, Waehneldt TV, Neuhoff V. The lipid composition of light and heavy myelin subfractions isolated from rabbit sciatic nerve. Neurosci. Lett 1980b;20:211–215. [PubMed: 7443071]

Londos C, Sztalryd C, Tansey JT, Kimmel AR. Role of pat proteins in lipid metabolism. Biochimie 2005;87:45–49. [PubMed: 15733736]

Miranda PJ, Defronzo RA, Califf RM, Guyton JR. Metabolic syndrome: Definition, pathophysiology, and mechanisms. Am. Heart J 2005a;149:33–45. [PubMed: 15660032]

Miranda PJ, Defronzo RA, Califf RM, Guyton JR. Metabolic syndrome: Evaluation of pathological and therapeutic outcomes. Am. Heart J 2005b;149:20–32. [PubMed: 15660031]

Moller DE, Kaufman KD. Metabolic syndrome: a clinical and molecular perspective. Annu. Rev. Med 2005;56:45–62. [PubMed: 15660501]

Newberry EP, Xie Y, Kennedy S, Han X, Buhman KK, Luo J, Gross RW, Davidson NO. Decreased hepatic triglyceride accumulation and altered fatty acid uptake in mice with deletion of the liver fatty acid-binding protein gene. J. Biol. Chem 2003;278:51, 664–51, 672.

Pond CM. Long-term changes in adipose tissue in human disease. Proc. Nutr. Soc 2001;60:365–374. [PubMed: 11681811]

Rechthand E, Rapoport SI. Regulation of the microenvironment of peripheral nerve: Role of the blood–nerve barrier. Prog. Neurobiol 1987;28:303–343. [PubMed: 3295996]

Reina MA, Lopez A, De Andres JA. [Adipose tissue within peripheral nerves. Study of the human sciatic nerve.]. Rev. Esp. Anestesiol. Reanim 2002;49:397–402. [PubMed: 12455319]

Saltiel AR, Kahn CR. Insulin signalling and the regulation of glucose and lipid metabolism. Nature 2001;414:799–806. [PubMed: 11742412]

Schmidt RE, Modert CW, Yip HK, Johnson EM, Jr. Retrograde axonal transport of intravenously administered 125i-nerve growth factor in rats with streptozotocin-induced diabetes. Diabetes 1983;32:654–663. [PubMed: 6345245]

Sima AAF, Zhang W, Xu G, Sugimoto K, Guberski D, Yorek MA. A comparison of diabetic polyneuropathy in type ii diabetic bbzdr/wor rats and in type i diabetic bb/wor rats. Diabetologia 2000;43:786–793. [PubMed: 10907124]

Stolinski C. Structure and composition of the outer connective tissue sheaths of peripheral nerve. J. Anat 1995;186:123–130. [PubMed: 7649808]

Su X, Han X, Yang J, Mancuso DJ, Chen J, Bickel PE, Gross RW. Sequential ordered fatty acid α oxidation and δ9 desaturation are major determinants of lipid storage and utilization in differentiating adipocytes. Biochemistry 2004;43:5033–5044. [PubMed: 15109262]

Sunderland S. The adipose tissue of peripheral nerves. Brain 1945;68:118–124.

Sunderland S. The connective tissues of peripheral nerves. Brain 1965;88:841–854. [PubMed: 4285460]

Unger RH. Lipotoxic diseases. Annu. Rev. Med 2002;53:319–336. [PubMed: 11818477]

Verheijen MH, Chrast R, Burrola P, Lemke G. Local regulation of fat metabolism in peripheral nerves. Genes Dev 2003;17:2450–2464. [PubMed: 14522948]

Xiao HS, Huang QH, Zhang FX, et al. Identification of gene expression profile of dorsal root ganglion in the rat peripheral axotomy model of neuropathic pain. Proc. Natl Acad. Sci. USA 2002;99:8360–8365. [PubMed: 12060780]

Yao JK, Dyck PJ, Vanloon JA, Moyer TP. Free fatty acid composition of human and rat peripheral nerve. J. Neurochem 1981;36:1211–1218. [PubMed: 7205267]

Zhu X, Eichberg J. 1,2-diacylglycerol content and its arachidonyl-containing molecular species are reduced in sciatic nerve from streptozotocin-induced diabetic rats. J. Neurochem 1990;55:1087–1090. [PubMed: 2117050]

Zhu X, Eichberg J. Molecular species composition of glycerophospholipids in rat sciatic nerve and its alteration in streptozotocin-induced diabetes. Biochim. Biophys. Acta 1993;1168:1–12. [PubMed: 8504134]

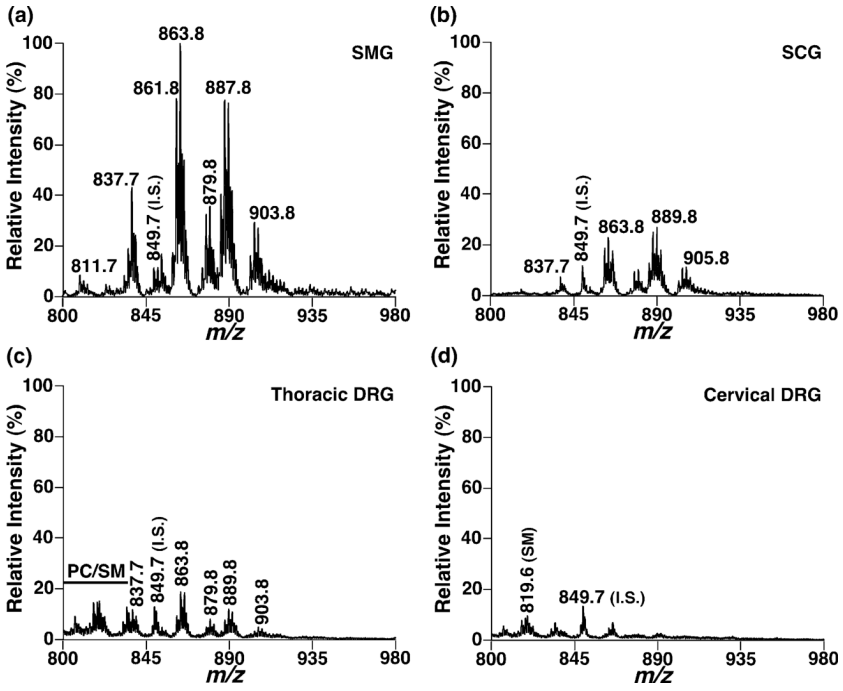

Fig. 1.

Representative positive-ion ESI/MS spectra of triacylglycerols in lipid extracts from rat ganglia. Rat ganglia including prevertebral superior mesenteric ganglia (a), paravertebral superior cervical ganglia (b), thoracic dorsal root ganglia (c) and cervical dorsal root ganglia (d) were dissected at 2 months of age. Lipids from these tissues were extracted using a modified Bligh and Dyer procedure as described in Materials and methods. All of the abundant ion peaks were identified using 2D mass spectrometry. The mass spectra in (b–d) were displayed after normalization to the internal standard peak in the mass spectrum in (a). All unspecified ion peaks are those of lithiated TAG molecular species. PC: phosphatidylcholine molecular species; SM: sphingomyelin; I.S.: internal standard of TAG.

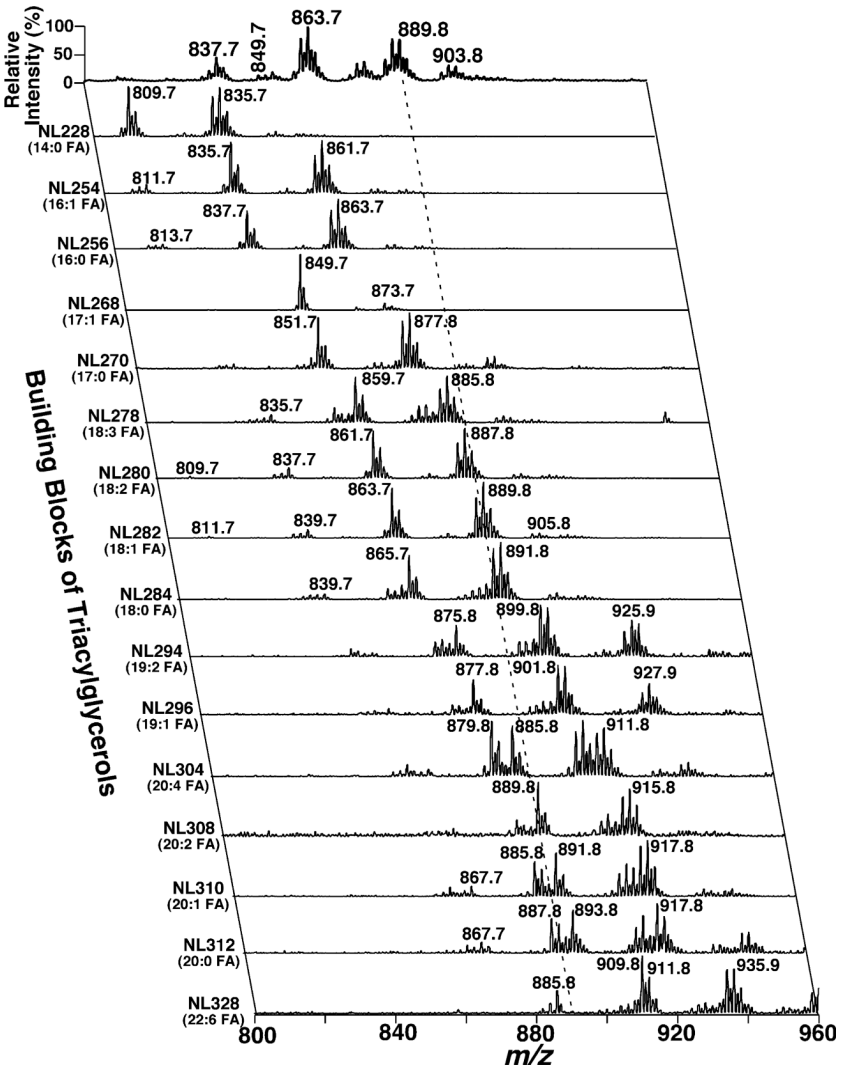

Fig. 2.

A representative two-dimensional ESI/MS analysis of triacylglycerol molecular species in rat superior mesenteric ganglial lipid extracts. The first dimension ESI mass spectrum was obtained (the topmost trace) in the positive-ion mode using intrasource separation. Next, neutral loss (NL) scans of all naturally-occurring aliphatic chains (i.e. the building blocks of TAG molecular species) of lipid extracts of rat superior mesenteric ganglia were acquired and used to identify the molecular species assignments, deconvolute isobaric molecular species and quantify triacylglycerol individual molecular species by comparisons with a selected internal standard. Each MS or MS/MS trace of the 2D ESI mass spectrum was acquired by sequentially programmed custom scans operating under XCALIBUR software as described in Materials and methods. All mass spectral traces were displayed after normalization to the base peak in the individual trace.

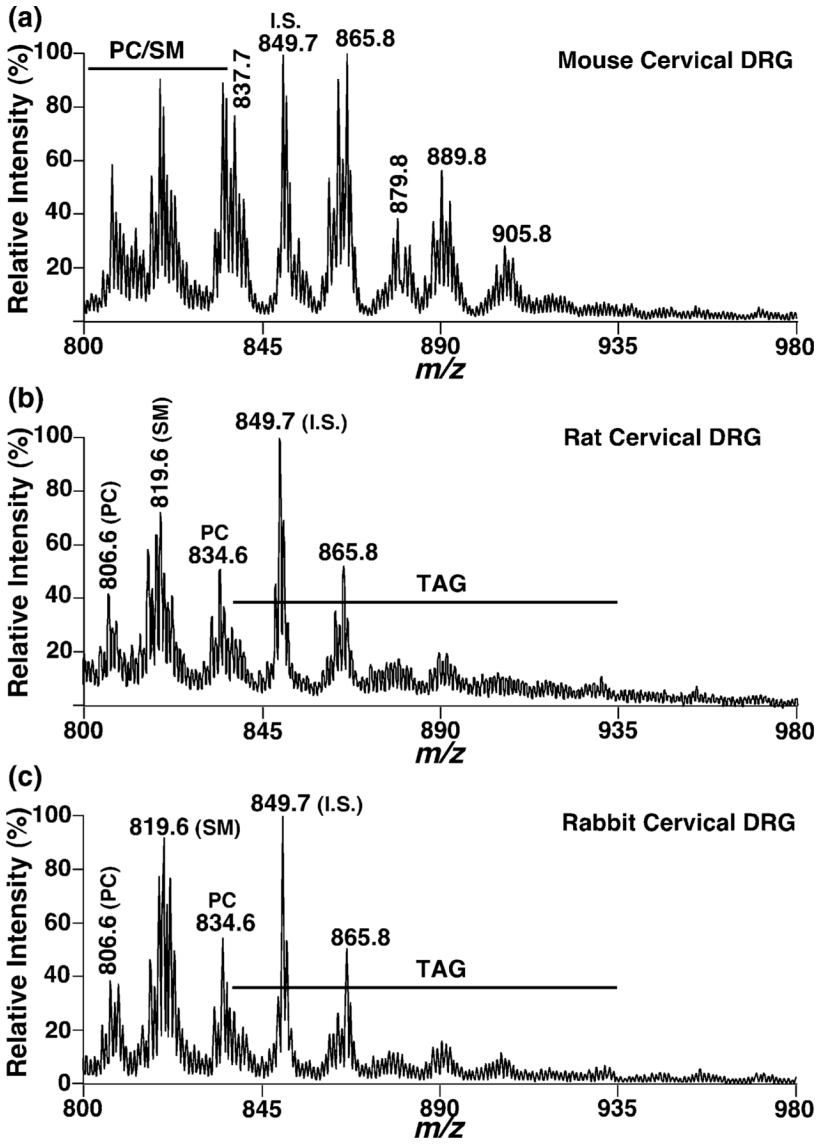

Fig. 3.

Representative positive-ion ESI/MS analyses of triacylglycerols in lipid extracts from cervical dorsal root ganglia of mouse, rat and rabbit. Mouse (a), rat (b) and rabbit (c) cervical DRG were dissected and lipids from these tissues were extracted by a modified Bligh and Dyer procedure. Ion peaks were identified using 2D mass spectrometric analyses as shown in Fig. 2 or described in Materials and methods. All unspecified ion peaks are those of lithiated TAG molecular species. PC: phosphatidylcholine molecular species; SM: sphingomyelin; I.S.: internal standard of TAG.

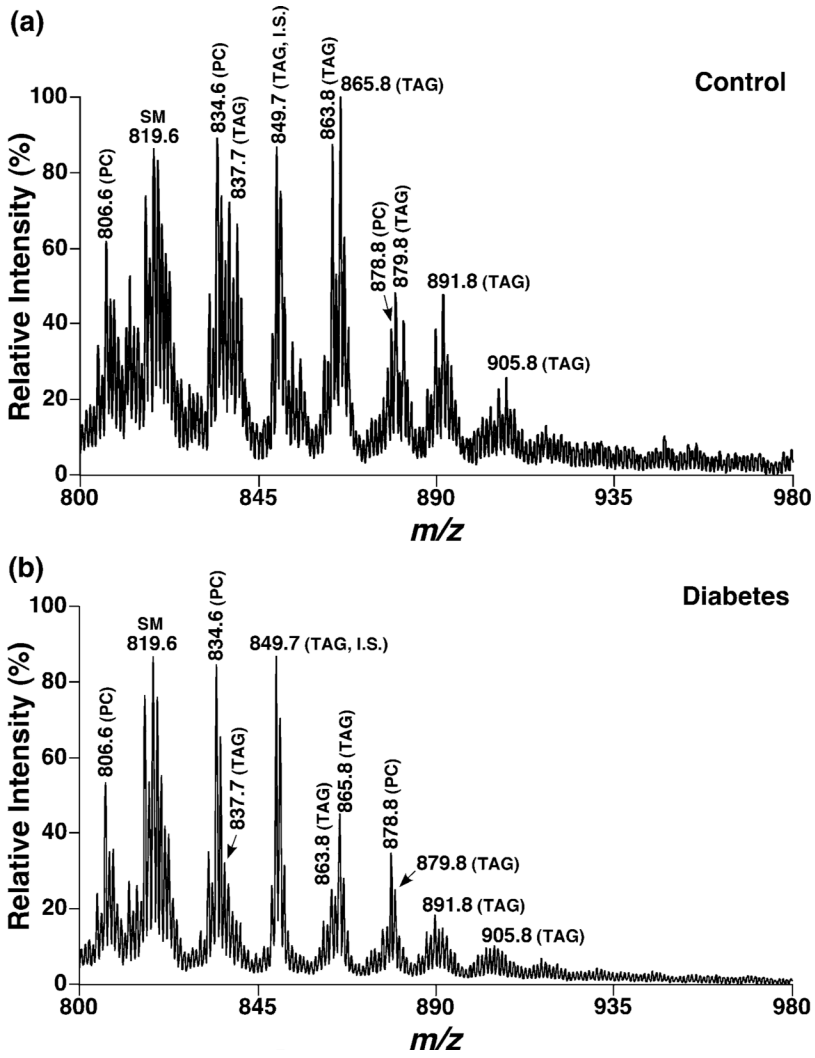

Fig. 4.

Representative ESI mass spectra of triacylglycerols in lipid extracts from cervical DRG of control and diabetic mice. Mice were rendered diabetic for 4 weeks by streptozotocin treatment at 4 months of age. Mouse cervical DRG were dissected and DRG lipids were extracted by a modified Bligh and Dyer procedure. TAG molecular ions were analyzed using positive-ion ESI/MS, and were further identified using 2D mass spectrometry as described in Materials and methods. The mass spectrum acquired from lipid extracts of diabetic mice DRG (b) has been normalized for the ion peak intensity of the TAG internal standard (I.S., *m/z* 849.7) relative to that of the control (a).

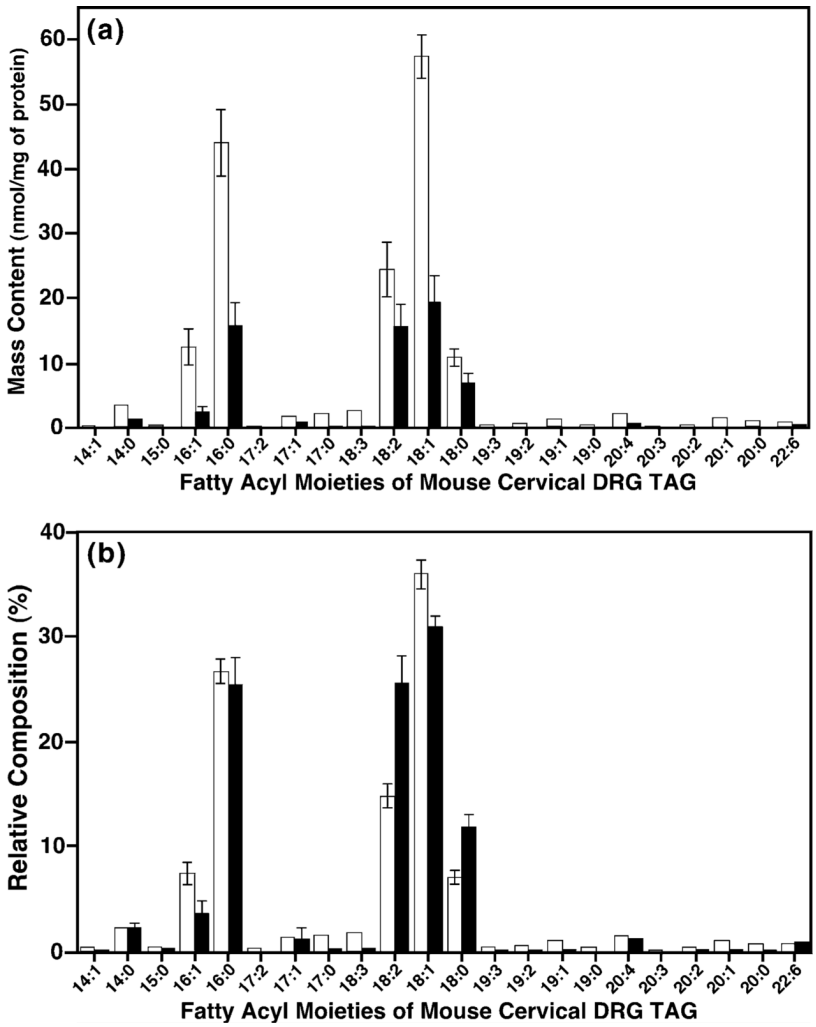

Fig. 5.

Alterations of the acyl chain composition of TAG in mouse cervical dorsal root ganglia induced by streptozotocin treatment. The acyl chain composition of TAG in mouse cervical DRG was quantitated from mass spectrometric analyses as described in Fig. 4. Each acyl chain moiety of the TAG from cervical DRG from diabetic (filled bars) and control (open bars) mice was compared in terms of either absolute mass content of each individual TAG fatty acyl chain (a) or relative composition of each individual TAG fatty acyl chain relative to the total acyl chains of TAG (b).

Table 1

Triacylglycerol molecular species and mass content in lipid extracts of rat ganglia[a]

$[M + Li]^+$	Molecular species	SMG	SCG	Thoracic DRG	Cervical DRG
807.7	T16 : 1	1.5 ± 0.1	0.3 ± 0.2	0.1 ± 0.1	0.1 ± 0.1
809.7	14 : 0/16 : 0/18 : 2, 16 : 0/16 : 1/16 : 1	6.7 ± 0.6	1.5 ± 0.4	0.5 ± 0.1	0.2 ± 0.1
811.7	14 : 0/16 : 0/18 : 1, 16 : 0/16 : 0/16 : 1	4.5 ± 0.4	1.2 ± 0.4	0.9 ± 0.1	0.4 ± 0.1
813.7	T16 : 0	3.9 ± 0.4	1.3 ± 0.3	0.8 ± 0.1	0.3 ± 0.1
823.7	15 : 0/16 : 1/18 : 1	2.2 ± 0.2	0.5 ± 0.1	0.1 ± 0.1	0.1 ± 0.1
833.7	14 : 0/18 : 1/18 : 3, 16 : 1/16 : 1/18 : 2,	6.1 ± 0.5	1.2 ± 0.2	1.4 ± 0.3	0.2 ± 0.1
835.7	14 : 0/18 : 1/18 : 2, 16 : 0/16 : 1/18 : 2, 16 : 1/16 : 1/18 : 1	16.8 ± 1.3	3.3 ± 0.6	1.3 ± 0.2	0.6 ± 0.1
837.7	14 : 0/18 : 0/18 : 2, 16 : 0/16 : 0/18 : 2, 16 : 0/16 : 1/18 : 1	41.6 ± 2.9	11.0 ± 1.2	4.2 ± 0.6	1.6 ± 0.1
839.7	16 : 0/16 : 0/18 : 1, 16 : 0/16 : 1/18 : 0	17.1 ± 1.1	5.0 ± 0.5	3.2 ± 0.3	1.4 ± 0.1
847.7	16 : 1/17 : 1/18 : 2	2.0 ± 0.2	0.4 ± 0.1	0.1 ± 0.1	
849.7	16 : 0/17 : 1/18 : 2, 16 : 1/17 : 1/18 : 1	3.5 ± 0.3	0.7 ± 0.1	0.2 ± 0.1	0.1 ± 0.1
851.7	16 : 1/17 : 0/18 : 1	4.1 ± 0.3	1.8 ± 0.1	0.6 ± 0.1	0.2 ± 0.1
853.7	14 : 1/18 : 3/20 : 4, 16 : 0/17 : 0/18 : 1	2.0 ± 0.2	0.9 ± 0.1	0.3 ± 0.1	0.1 ± 0.1
857.7	16 : 1/18 : 2/18 : 3	1.5 ± 0.1	0.3 ± 0.1	0.1 ± 0.1	0.1 ± 0.1
859.8	16 : 0/16 : 1/20 : 4, 16 : 1/18 : 2/18 : 2	15.1 ± 1.2	3.0 ± 0.3	0.6 ± 0.1	0.3 ± 0.1
861.8	16 : 0/18 : 2/18 : 2, 16 : 1/18 : 1/18 : 2	72.5 ± 6.5	17.1 ± 0.2	3.4 ± 0.4	1.3 ± 0.1
863.8	16 : 0/18 : 1/18 : 2, 16 : 1/18 : 0/18 : 2, 16 : 1/18 : 1/18 : 1	83.2 ± 5.8	21.6 ± 1.0	7.5 ± 0.8	3.0 ± 0.2
865.8	16 : 0/18 : 0/18 : 2, 16 : 0/18 : 1/18 : 1	31.8 ± 2.9	11.4 ± 0.7	6.0 ± 0.4	2.2 ± 0.2
867.8	16 : 0/18 : 0/18 : 1	4.4 ± 0.3	2.5 ± 0.2	1.4 ± 0.1	0.6 ± 0.1
873.8	17 : 1/18 : 2/18 : 2	1.3 ± 0.1	0.5 ± 0.1	0.3 ± 0.1	0.2 ± 0.1
875.8	17 : 1/18 : 1/18 : 2	3.4 ± 0.3	1.1 ± 0.1	0.2 ± 0.1	0.1 ± 0.1
877.8	17 : 0/18 : 1/18 : 2	3.2 ± 0.3	1.2 ± 0.1	0.2 ± 0.1	0.6 ± 0.1
879.8	17 : 0/18 : 1/18 : 1	2.2 ± 0.2	0.8 ± 0.1	0.2 ± 0.1	0.1 ± 0.1
881.8	17 : 0/18 : 0/18 : 1	1.3 ± 0.1	0.6 ± 0.1	0.2 ± 0.1	0.1 ± 0.1
883.8	16 : 1/18 : 2/20 : 4	5.0 ± 0.4	1.3 ± 0.1	0.2 ± 0.1	0.1 ± 0.1
885.8	16 : 0/18 : 2/20 : 4, T18 : 2	35.6 ± 3.2	8.9 ± 0.8	1.1 ± 0.1	0.4 ± 0.1
887.8	16 : 0/18 : 1/20 : 4, 18 : 0/18 : 2/18 : 3, 18 : 1/18 : 2/18 : 2	62.7 ± 4.9	16.9 ± 2.1	3.1 ± 0.2	1.1 ± 0.1
889.8	18 : 0/18 : 2/18 : 2, 18 : 1/18 : 1/18 : 2	55.5 ± 4.8	18.4 ± 1.5	4.9 ± 0.3	1.7 ± 0.1
891.8	16 : 0/18 : 2/20 : 1, 18 : 0/18 : 1/18 : 2, T18 : 1	25.9 ± 2.3	11.5 ± 0.8	4.1 ± 0.3	1.4 ± 0.1
893.8	16 : 0/18 : 1/20 : 1, 18 : 0/18 : 1/18 : 1	6.3 ± 0.5	4.4 ± 0.2	1.7 ± 0.1	0.6 ± 0.1
901.8	17 : 0/18 : 3/19 : 2	1.5 ± 0.2	0.5 ± 0.1	0.1 ± 0.1	
903.8	18 : 0/18 : 3/19 : 1	1.8 ± 0.2	0.7 ± 0.1	0.1 ± 0.1	
905.8	16 : 1/18 : 3/22 : 6, 18 : 1/18 : 2/19 : 0	1.4 ± 0.1	0.6 ± 0.1	0.2 ± 0.1	
909.8	18 : 2/18 : 2/20 : 4	4.1 ± 0.3	1.3 ± 0.1	0.2 ± 0.1	0.1 ± 0.1
911.8	16 : 0/18 : 1/22 : 6, 18 : 1/18 : 2/20 : 4	6.0 ± 0.5	2.0 ± 0.2	0.5 ± 0.1	0.3 ± 0.1
913.8	18 : 1/18 : 1/20 : 4, 18 : 2/18 : 2/20 : 2	5.6 ± 0.4	2.2 ± 0.3	0.6 ± 0.1	0.2 ± 0.1
915.8	18 : 1/18 : 2/20 : 2, 18 : 2/18 : 2/20 : 1	4.3 ± 0.4	1.8 ± 0.1	0.6 ± 0.1	0.2 ± 0.1
917.8	18 : 1/18 : 2/20 : 1	3.8 ± 0.3	1.3 ± 0.1	0.5 ± 0.1	0.1 ± 0.1
919.8	18 : 0/18 : 2/20 : 1	1.7 ± 0.2	0.8 ± 0.1	0.4 ± 0.1	0.1 ± 0.1
935.8	18 : 1/18 : 2/22 : 6	1.3 ± 0.1	0.7 ± 0.1	0.1 ± 0.1	
	Total TAG	543.3 ± 44.6	167.0 ± 13.6	53.1 ± 3.9	22.0 ± 2.5
	16 : 0 FA	396.8 ± 43.5 (23.4 ± 2.1)	104.2 ± 11.0 (20.7 ± 1.6)	42.7 ± 3.8 (26.8 ± 2.4)	14.9 ± 1.9 (22.6 ± 2.8)
	18 : 0 FA	116.7 ± 8.5 (6.9 ± 0.5)	55.8 ± 2.9 (11.2 ± 0.8)	15.9 ± 0.5 (10.0 ± 0.3)	5.6 ± 1.0 (8.4 ± 1.5)
	18 : 1 FA	525.1 ± 37.1 (30.9 ± 2.8)	127.7 ± 0.3 (25.5 ± 0.6)	48.5 ± 3.4 (30.5 ± 2.1)	16.3 ± 2.1 (24.1 ± 3.2)
	18 : 2 FA	425.3 ± 32.0 (25.0 ± 2.3)	141.4 ± 5.6 (28.4 ± 1.7)	26.7 ± 2.5 (16.7 ± 1.5)	9.3 ± 1.3 (14.1 ± 2.0)
	Odd numbered FA	46.5 ± 4.8 (2.7 ± 0.4)	19.2 ± 0.9 (3.9 ± 0.5)	7.9 ± 1.3 (5.0 ± 0.8)	3.8 ± 0.7 (5.7 ± 1.1)
	Polyunsaturated FA[b]	520.1 ± 40.6 (30.6 ± 2.9)	175.4 ± 8.4 (35.1 ± 2.1)	35.0 ± 2.8 (22.0 ± 1.7)	15.3 ± 1.9 (23.1 ± 2.9)
	FA w/20 or 22 carbons	67.1 ± 4.8 (4.0 ± 1.0)	25.8 ± 2.9 (5.1 ± 0.5)	8.1 ± 0.6 (5.1 ± 0.4)	3.9 ± 0.6 (5.9 ± 0.9)

[a] Rat ganglial lipids were extracted by a modified Bligh and Dyer procedure and the TAG molecular species in the lipid extracts were identified and quantified using a 2D ESI mass spectrometric technique as described in the Materials and methods. The results are expressed in nmol/mg of protein and represent X ± SEM of at least four different rats at 2 months of age, whereas the data in

J Neurochem. Author manuscript; available in PMC 2007 December 13.

parentheses are the percentages of the acyl chains in the TAG molecular species. SMG: prevertebral superior mesenteric ganglia; SCG: paravertebral superior cervical ganglia; DRG: dorsal root ganglia; FA: fatty acyl chain. Only the TAG molecular species that contribute over 0.2 mol% of total SMG TAG in rats are listed in the Table.

[b] Acyl chains in TAG molecular species containing two or more double bonds.

Table 2

Triacylglycerol molecular species and mass content in lipid extracts of mouse cervical dorsal root ganglia at different ages[a]

[M + Li]$^+$	Major species	2 months	5 months	8 months
783.7	14 : 0/16 : 0/16 : 1	0.3 ± 0.1	0.3 ± 0.1	0.2 ± 0.1
809.7	14 : 0/16 : 0/18 : 2, 16 : 0/16 : 1/16 : 1	0.9 ± 0.1	1.1 ± 0.2	1.0 ± 0.1
811.7	14 : 0/16 : 0/18 : 1, 16 : 0/16 : 0/16 : 1	1.9 ± 0.1	1.6 ± 0.2	1.6 ± 0.2
813.7	T16 : 0	0.8 ± 0.1	0.6 ± 0.1	0.8 ± 0.2
833.7	16 : 1/16 : 1/18 : 2	0.4 ± 0.1	0.5 ± 0.1	0.4 ± 0.1
835.7	14 : 0/18 : 1/18 : 2, 16 : 0/16 : 1/18 : 2, 16 : 1/16 : 1/18 : 1	2.8 ± 0.2	2.8 ± 0.3	1.9 ± 0.1
837.7	14 : 0/18 : 0/18 : 2, 16 : 0/16 : 0/18 : 2, 16 : 0/16 : 1/18 : 1	4.9 ± 0.1	5.2 ± 0.4	4.5 ± 0.3
839.7	16 : 0/16 : 0/18 : 1, 16 : 0/16 : 1/18 : 0	4.6 ± 0.3	3.2 ± 0.2	3.0 ± 0.3
853.7	16 : 0/17 : 0/18 : 1	0.3 ± 0.1	0.3 ± 0.1	0.3 ± 0.1
859.8	16 : 0/16 : 1/20 : 4, 16 : 1/18 : 2/18 : 2	0.7 ± 0.1	0.9 ± 0.1	0.6 ± 0.1
861.8	16 : 0/18 : 2/18 : 2, 16 : 1/18 : 1/18 : 2	3.6 ± 0.2	3.5 ± 0.3	2.7 ± 0.2
863.8	16 : 0/18 : 1/18 : 2, 16 : 1/18 : 0/18 : 2, 16 : 1/18 : 1/18 : 1	6.8 ± 0.4	7.2 ± 0.6	5.0 ± 0.3
865.8	16 : 0/18 : 0/18 : 2, 16 : 0/18 : 1/18 : 1	6.4 ± 0.5	6.0 ± 0.4	4.2 ± 0.4
867.8	16 : 0/18 : 0/18 : 1	1.0 ± 0.3	0.7 ± 0.1	0.7 ± 0.1
873.8	17 : 1/18 : 2/18 : 2	0.6 ± 0.1	0.4 ± 0.1	0.5 ± 0.1
885.8	16 : 0/18 : 2/20 : 4, T18 : 2	0.8 ± 0.1	0.8 ± 0.1	0.7 ± 0.1
887.8	16 : 0/18 : 1/20 : 4, 18 : 0/18 : 2/18 : 3, 18 : 1/18 : 2/18 : 2	2.5 ± 0.1	2.5 ± 0.2	2.0 ± 0.2
889.8	18 : 0/18 : 2/18 : 2, 18 : 1/18 : 1/18 : 2	4.6 ± 0.2	4.2 ± 0.4	3.1 ± 0.2
891.8	16 : 0/18 : 2/20 : 1, 18 : 0/18 : 1/18 : 2, T18 : 1	4.7 ± 0.3	4.6 ± 0.4	2.2 ± 0.2
893.8	16 : 0/18 : 1/20 : 1, 18 : 0/18 : 1/18 : 1	1.5 ± 0.2	0.9 ± 0.1	0.6 ± 0.1
911.8	16 : 0/18 : 1/22 : 6	0.3 ± 0.1	0.3 ± 0.1	0.3 ± 0.1
915.8	18 : 0/18 : 1/20 : 4	0.4 ± 0.1	0.3 ± 0.1	0.3 ± 0.1
919.8	18 : 1/18 : 1/20 : 1	0.3 ± 0.1	0.3 ± 0.1	0.2 ± 0.1
	Total TAG[b]	55.5 ± 2.4	49.9 ± 5.3*	41.7 ± 3.0**
	16 : 0 FA	46.3 ± 1.9 (27.8 ± 1.2)	37.3 ± 5.5 (24.9 ± 3.7)	35.6 ± 4.3 (28.5 ± 3.5)
	18 : 0 FA	15.0 ± 2.2 (9.0 ± 1.3)	12.3 ± 0.6 (8.2 ± 0.4)	8.2 ± 1.9 (6.5 ± 1.9)
	18 : 1 FA	50.4 ± 3.2 (30.3 ± 1.9)	49.2 ± 4.2 (32.9 ± 2.8)	35.8 ± 1.4 (28.6 ± 1.1)
	18 : 2 FA	20.8 ± 1.6 (12.5 ± 0.9)	20.7 ± 2.8 (13.8 ± 1.9)	18.8 ± 2.0 (15.0 ± 1.6)
	Odd numbered FA	9.4 ± 0.2 (5.7 ± 0.2)	8.5 ± 0.8 (5.7 ± 0.6)	7.3 ± 0.7 (5.8 ± 0.6)
	Polyunsaturated FA[c]	31.3 ± 1.5 (18.8 ± 1.0)	29.4 ± 3.1 (19.6 ± 2.1)	25.8 ± 1.5 (20.6 ± 1.2)
	FA w/20 or 22 carbons	7.8 ± 0.7 (4.7 ± 0.4)	6.8 ± 0.6 (4.6 ± 0.4)	5.4 ± 0.7 (4.3 ± 0.5)

[a] Mouse cervical DRG lipids were extracted by a modified Bligh and Dyer procedure and the TAG molecular species in the lipid extracts were identified and quantified using a 2D ESI mass spectrometric technique as described in the Materials and methods. The results are expressed in nmol/mg of protein and represent X ± SEM of at least four different animals, whereas the data in parentheses are the percentages of the acyl chains in TAG molecular species. FA: fatty acyl chain. Only the TAG molecular species that contribute over 0.5 mol% of total DRG TAG in mice at 2 months of age are listed in the Table.

[b] $p < 0.05$ and

* $p < 0.05$ and

** $p < 0.001$ relative to values at 2 months.

[c] Acyl chains in TAG molecular species containing two or more double bonds.

Table 3

Triacylglycerol molecular species and mass content in lipid extracts of cervical dorsal root ganglia of control and diabetic mice[a]

[M + Li]$^+$	Major species	Control	Diabetes
783.7	14 : 0/16 : 0/16 : 1	0.3 ± 0.1	0.1 ± 0.1
809.7	14 : 0/16 : 0/18 : 2, 16 : 0/16 : 1/16 : 1	1.1 ± 0.2	0.2 ± 0.1
811.7	14 : 0/16 : 0/18 : 1, 16 : 0/16 : 0/16 : 1	1.6 ± 0.2	0.4 ± 0.1
813.7	T16 : 0	0.62 ± 0.08	0.25 ± 0.03
833.7	16 : 1/16 : 1/18 : 2	0.48 ± 0.06	0.18 ± 0.02
835.7	14 : 0/18 : 1/18 : 2, 16 : 0/16 : 1/18 : 2, 16 : 1/16 : 1/18 : 1	2.8 ± 0.3	0.8 ± 0.1
837.7	14 : 0/18 : 0/18 : 2, 16 : 0/16 : 0/18 : 2, 16 : 0/16 : 1/18 : 1	5.2 ± 0.4	1.9 ± 0.2
839.7	16 : 0/16 : 0/18 : 1, 16 : 0/16 : 1/18 : 0	3.2 ± 0.2	1.1 ± 0.1
853.7	16 : 0/17 : 0/18 : 1	0.31 ± 0.06	0.05 ± 0.01
859.8	16 : 0/16 : 1/20 : 4, 16 : 1/18 : 2/18 : 2	0.9 ± 0.1	0.3 ± 0.1
861.8	16 : 0/18 : 2/18 : 2, 16 : 1/18 : 1/18 : 2	3.5 ± 0.3	1.7 ± 0.1
863.8	16 : 0/18 : 1/18 : 2, 16 : 1/18 : 0/18 : 2, 16 : 1/18 : 1/18 : 1	7.2 ± 0.6	2.6 ± 0.3
865.8	16 : 0/18 : 0/18 : 2, 16 : 0/18 : 1/18 : 1	6.0 ± 0.4	1.7 ± 0.2
867.8	16 : 0/18 : 0/18 : 1	0.54 ± 0.06	0.32 ± 0.03
873.8	17 : 1/18 : 2/18 : 2	0.35 ± 0.05	0.15 ± 0.02
885.8	16 : 0/18 : 2/20 : 4, T18 : 2	0.8 ± 0.1	0.5 ± 0.1
887.8	16 : 0/18 : 1/20 : 4, 18 : 0/18 : 2/18 : 3, 18 : 1/18 : 2/18 : 2	2.5 ± 0.2	1.2 ± 0.1
889.8	18 : 0/18 : 2/18 : 2, 18 : 1/18 : 1/18 : 2	4.2 ± 0.4	2.3 ± 0.2
891.8	16 : 0/18 : 2/20 : 1, 18 : 0/18 : 1/18 : 2, T18 : 1	4.6 ± 0.4	1.8 ± 0.2
893.8	16 : 0/18 : 1/20 : 1, 18 : 0/18 : 1/18 : 1	0.9 ± 0.1	0.4 ± 0.1
911.8	16 : 0/18 : 1/22 : 6	0.30 ± 0.03	0.16 ± 0.02
915.8	18 : 0/18 : 1/20 : 4	0.31 ± 0.05	0.18 ± 0.02
919.8	18 : 1/18 : 1/20 : 1	0.29 ± 0.03	0.09 ± 0.01
	Total TAG[b]	49.9 ± 5.3	22.0 ± 4.7[**]
	16 : 0 FA	37.3 ± 5.5 (24.9 ± 3.7)	15.6 ± 3.5 (23.9 ± 2.5)
	18 : 0 FA	12.3 ± 0.6 (8.2 ± 0.4)	7.1 ± 1.4 (11.1 ± 1.2)
	18 : 1 FA	49.2 ± 4.2 (32.9 ± 2.9)	19.4 ± 4.3 (29.1 ± 1.0)
	18 : 2 FA	20.7 ± 2.8 (13.8 ± 1.9)	15.9 ± 3.6 (24.2 ± 2.5)
	Odd-numbered FA	8.5 ± 0.8 (5.7 ± 0.6)	2.2 ± 0.8 (3.7 ± 1.4)
	Polyunsaturated FA[c]	29.4 ± 3.1 (19.6 ± 2.1)	17.4 ± 4.4 (26.6 ± 3.1)
	FA w/20 or 22 carbons	6.8 ± 0.6 (4.6 ± 0.4)	1.5 ± 0.5 (2.2 ± 0.4)

[a] Mouse diabetes was induced by streptozotocin treatment. Lipids of mouse cervical dorsal root ganglia (DRG) were extracted using a modified Bligh and Dyer procedure and the TAG molecular species in the lipid extracts were identified and quantified by the 2D ESI mass spectrometric approach after intrasource separation as described in the Materials and methods. The results are expressed in nmol/mg of protein and represent X ± SEM of a minimum of four different animals. Only the TAG molecular species that contribute over 0.5 mol% of total DRG TAG in control mice are listed in the Table.

[b] $p < 0.001$ relative to values in controls.

[**] $p < 0.001$ relative to values in controls.

[c] Acyl chains in TAG molecular species containing two or more double bonds.